Acta Cryst E CRYSTALLOGRAPHIC COMMUNICATIONS

ISSN 2056-9890

Methyl 3-[(1-benzyl-4-phenyl-1*H*-1,2,3-triazol-5-yl)formamido]propanoate: crystal structure, Hirshfeld surface analysis and computational chemistry

Ignez Caracelli,[a]* Julio Zukerman-Schpector,[b] Huey Chong Kwong[c] and Edward R. T. Tiekink[c]‡

[a]Departmento de Física, Universidade Federal de São Carlos, 13565-905 São Carlos, SP, Brazil, [b]Laboratório de Cristalografia, Esterodinâmica e Modelagem Molecular, Departamento de Química, Universidade Federal de São Carlos, 13565-905 São Carlos, SP, Brazil, and [c]Research Centre for Crystalline Materials, School of Science and Technology, Sunway University, 47500 Bandar Sunway, Selangor Darul Ehsan, Malaysia. *Correspondence e-mail: ignez@df.ufscar.br

Received 28 May 2020
Accepted 3 June 2020

Edited by W. T. A. Harrison, University of Aberdeen, Scotland

‡ Additional correspondence author, e-mail: edwardt@sunway.edu.my.

Keywords: crystal structure; 1,2,3-triazole; Hirshfeld surface analysis; computational chemistry.

CCDC reference: 2007664

Supporting information: this article has supporting information at journals.iucr.org/e

The title compound, $C_{20}H_{20}N_4O_3$, is constructed about a tri-substituted 1,2,3-triazole ring, with the substituent at one C atom flanked by the C and N atoms being a substituted amide group, and with the adjacent C and N atoms bearing phenyl and benzyl groups, respectively; the dihedral angle between the pendant phenyl rings is 81.17 (12)°, indicative of an almost orthogonal disposition. In the crystal, pairwise amide-N—H···O(carbonyl) hydrogen bonds lead to a centrosymmetric dimer incorporating methylene-C—H···π(benzene) interactions. The dimers are linked into a supramolecular layer in the *ab* plane *via* methylene-C—H···N(azo) and benzene-C—H···O(amide) interactions; the layers stack along the *c*-axis direction without directional interactions between them. The above-mentioned intermolecular contacts are apparent in the analysis of the calculated Hirshfeld surface, which also provides evidence for short interlayer H···C contacts with a significant dispersion energy contribution.

1. Chemical context

The title 1,2,3-triazole-5-carboxamide derivative, (I), was recently prepared and characterized from a palladium-catalysed aminocarbonylation reaction with the use of dimethyl carbonate as a sustainable solvent (de Albuquerque *et al.*, 2019). The motivation for preparing such molecules rests with the known pharmacological activity of these and related 1,2,3-triazole derivatives (Bonandi *et al.*, 2017). Unambiguous structure determination of (I) is reported herein, *via* X-ray crystallography, as is a detailed analysis of the supramolecular association by Hirshfeld surface analysis and computational chemistry.

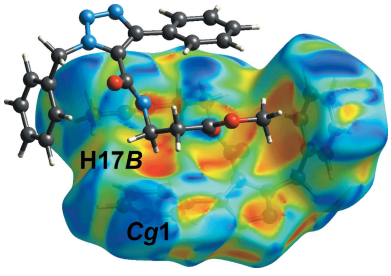

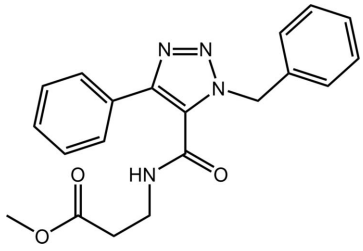

2. Structural commentary

The molecular structure of (I), Fig. 1, features a tri-substituted 1,2,3-triazole ring. The five-membered ring is strictly planar

Table 1
Hydrogen-bond geometry (Å, °).

*Cg*1 is the centroid of the (C10–C15) ring.

D—H···*A*	*D*—H	H···*A*	*D*···*A*	*D*—H···*A*
N4—H4*N*···O2^{i}	0.86 (3)	2.04 (3)	2.884 (4)	167 (3)
C3—H3*B*···N2^{ii}	0.97	2.55	3.495 (5)	165
C15—H15···O1^{iii}	0.93	2.51	3.335 (5)	148
C17—H17*B*···*Cg*1^{i}	0.97	2.71	3.640 (4)	161

Symmetry codes: (i) $-x+1, -y, -z+1$; (ii) $-x, -y+1, -z+1$; (iii) $-x+1, -y+1, -z+1$.

with the r.m.s. deviation of the fitted atoms being 0.0021 Å. Within the ring, the lengthening of the formal azo-N2—N3 [1.306 (4) Å] and C1—C2 [1.388 (4) Å] double bonds coupled with the shortening of the N1—N2 [1.341 (4) Å], C1—N3 [1.368 (4) Å] and C2—N1 [1.347 (4) Å] bonds from their standard double/single bond values, are indicative of significant delocalization of π-electron density over the ring atoms. While the N1-bound C3-atom lies 0.131 (6) Å out of the plane of the ring, the C1- and C2-bound C10 [0.012 (6) Å] and C16 [0.008 (6) Å] atoms are effectively co-planar with the ring. The terminal residues are twisted out of the plane of the central ring as seen in the (C1,C2,N1–N3)/(C4–C9) [74.46 (13)°], (C1,C2,N1–N3)/(C10–C15) [28.10 (17)°] and (C1,C2,N1–N3)/(C16,N4,O1) [47.1 (2)°] dihedral angles. The dihedral angle between the terminal phenyl rings is 81.17 (12)° indicating a close to orthogonal disposition. There is a twist in the amide residue as seen in the value of the N4—C17—C18—C19 torsion angle of 73.6 (4)°, indicating a (+)*syn*-clinal relationship. This results in a dihedral angle close to orthogonal for the amide (C16,N4,O1) and carboxylate (C19,O2,O3) residues, *i.e.* 73.6 (4)°.

3. Supramolecular features

The molecular packing in (I) features several identifiable points of contact, Table 1. The most evident of these are amide-N4—H···O2(carbonyl) hydrogen bonds occurring between centrosymmetrically related molecules to give the dimer shown in Fig. 2(*a*). The molecules in the dimer are linked *via* a 12-membered $\{\cdots OC_3NH\}_2$ synthon and additional stability to the assembly is provided by methylene-C17—H···π(benzene) interactions. The dimeric aggregates are connected into a supramolecular layer propagating in the *ab* plane *via* methylene-C3—H···N2(azo) and benzene-C15—H···O1(amide) interactions, Fig. 2(*b*). The layers stack in an ...*ABAB*... pattern along the *c* axis and inter-digitate to potentially form π–π interactions. However, these are not apparent, Fig. 2(*c*). A more detailed analysis of the interactions occurring in the inter-layer region is provided by an analysis of the calculated Hirshfeld surfaces.

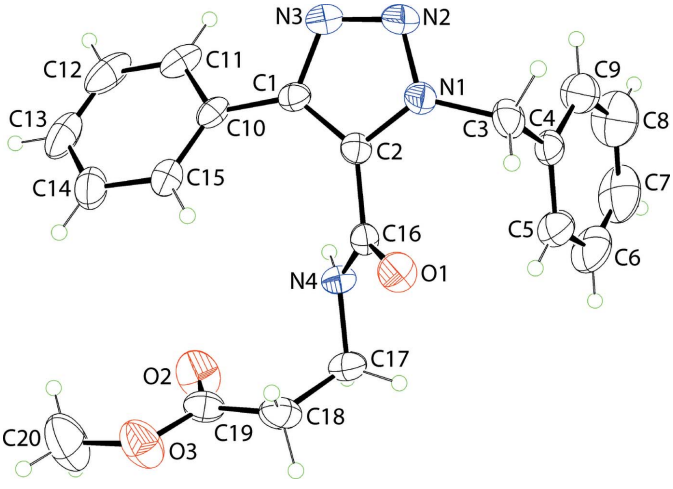

Figure 1
The molecular structure of (I), showing the atom-labelling scheme and displacement ellipsoids at the 35% probability level.

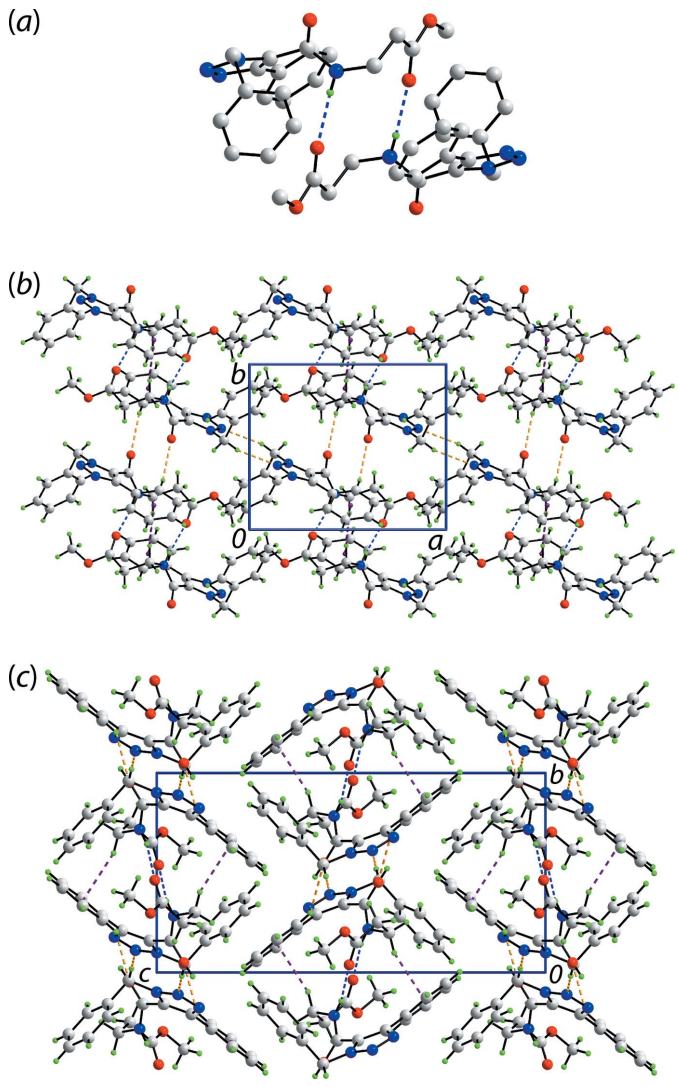

Figure 2
Molecular packing in (I): (*a*) supramolecular dimer sustained by amide-N4—H···O2(carbonyl) hydrogen bonds (H atoms omitted for clarity), (*b*) layer where the dimers of (*a*) are connected by methylene-C3—H···N(azo) and benzene-C15—H···O1(amide) interactions [the methylene-C17—H···π(benzene) interactions occur within the dimers] and (*c*) a view of the unit-cell contents shown in projection down the *a* axis. The N—H···O, C—H···O and C—H···π interactions are shown as blue, orange and purple dashed lines, respectively.

Table 2
Summary of short interatomic contacts (Å) in (I)[a].

Contact	Distance	Symmetry operation
H4*N*···O2[b]	1.90	$-x+1, -y, -z+1$
H3*B*···N2[b]	2.44	$-x+1, -y+1, -z+1$
H15···O1[b]	2.38	$-x, -y+1, -z+1$
H7···C5	2.63	$-x, y-\frac{1}{2}, -z+\frac{1}{2}$
H17*A*···C12	2.72	$x, -y+\frac{1}{2}, z-\frac{1}{2}$
H12···C15	2.73	$-x+1, y-\frac{1}{2}, -z+\frac{3}{2}$

Notes: (*a*) The interatomic distances are calculated in *Crystal Explorer 17* (Turner *et al.*, 2017) whereby the *X*—H bond lengths are adjusted to their neutron values. (*b*) These interactions correspond to those reported in Table 1.

4. Hirshfeld surface analysis

In order to probe the interaction between molecules of (I) in the crystal, Hirshfeld surfaces mapped with the normalized contact distance d_{norm} (McKinnon *et al.*, 2004), electrostatic potential (Spackman *et al.*, 2008) and two-dimensional fingerprint plots were calculated using *Crystal Explorer 17* (Turner *et al.*, 2017) by established procedures (Tan *et al.*, 2019). The electrostatic potentials were calculated using the wavefunction at the HF/STO-3 G level of theory. The bright-red spots on the Hirshfeld surface mapped over d_{norm} in Fig. 3(*a*), *i.e.* near the amide-H4*N* and carbonyl-O2 atoms, correspond to the amide-N—H4*N*···O2(carbonyl) hydrogen bond (Table 1). This hydrogen bond is also reflected in Hirshfeld surface mapped over the electrostatic potential Fig. 3(*b*), where the blue (positive electrostatic potential) and red (negative electrostatic potential) regions are apparent around the amide-H4*N* and carbonyl-O2 atoms, respectively.

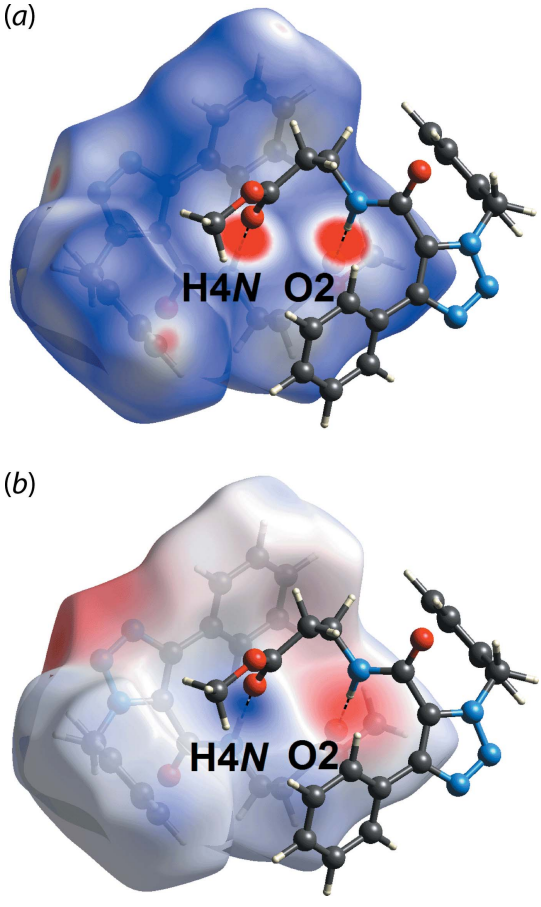

Figure 3
Views of the Hirshfeld surface for (I) mapped over (*a*) d_{norm} in the range −0.249 to +1.397 arbitrary units and (*b*) the electrostatic potential map in the range −0.097 to 0.134 atomic units, highlighting N—H···O hydrogen bonding.

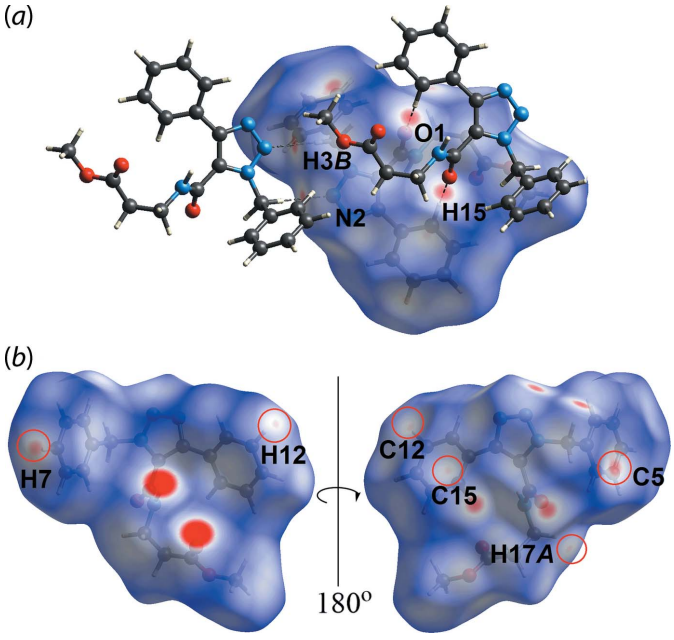

Figure 4
Views of the Hirshfeld surface mapped over d_{norm} for (I) in the range −0.249 to +1.397 arbitrary units, highlighting (*a*) weak C—H···N and C—H···O interactions and (*b*) short H···C contacts, highlighted within red circles.

The methylene-C3—H···N2(azo) and benzene-C15—H15···O1(amide) interactions are observed as faint-red spots on the d_{norm}-mapped Hirshfeld surface in Fig. 4(*a*), with a distance of ∼0.3 Å shorter than the sum of their van der Waals radii, Table 2. The other faint red spots near the benzyl (C5, C12, C15, H7 and H12) and methylene (H17*A*) atoms in

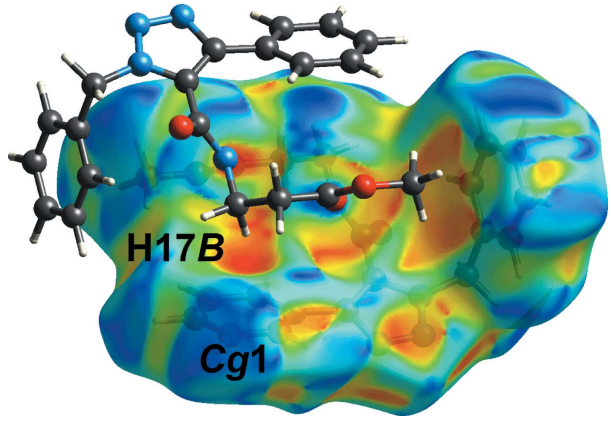

Figure 5
A view of the Hirshfeld surface for (I) mapped with the shape-index property, highlighting the intermolecular C—H···π interaction.

Table 3
Percentage contributions of interatomic contacts to the Hirshfeld surface for (I).

Contact	Percentage contribution
H···H	46.7
H···C/C···H	24.9
H···O/O···H	14.4
H···N/N···H	12.6
O···C/C···O	1.0
O···O	0.4

Fig. 4(*b*) correspond to the inter-layer H7···C5, H17*A*···C12 and H12···C15 short contacts listed in Table 2. Even though the C—H···π interaction, Table 1, was not manifested on the d_{norm}-mapped Hirshfeld surface, this interaction shows up as a distinctive orange 'pothole' on the shape-index-mapped Hirshfeld surface, Fig. 5.

The overall two-dimensional fingerprint plot for the Hirshfeld surface of (I) is shown with characteristic pseudo-symmetric wings in the upper left and lower right sides of the d_e and d_i diagonal axes, respectively, in Fig. 6(*a*). The delineated H···H, H···C/C···H, H···O/O···H and H···N/N···H contacts from the overall two-dimensional fingerprint plot are illustrated in Fig. 6(*b*)–(*e*), respectively. The percentage contributions from different interatomic contacts to the Hirshfeld surface of (I) are summarized in Table 3. The greatest contribution to the overall Hirshfeld surface are due to H···H contacts, which contribute 46.7%. However, the H···H contacts appear as a square-like distribution with a small beak at $d_e = d_i$ ~2.6 Å in Fig. 6(*b*), corresponding to H8···H11 ≃2.67 Å (symmetry operation: $-x$, $-y$, $-z + 1$) indicating that all H···H contacts have long-range characteristics. The H···C/C···H contacts on the Hirshfeld surface, which contribute 24.9% to the overall surface, Fig. 6(*c*), reflect the C—H···π interaction and C···H short contacts as discussed above. Consistent with the C—H···O and C—H···N interactions occurring in the crystal, H···O/O···H and H···N/N···H contacts contribute 14.4 and 12.6%, respectively, to the overall Hirshfeld surface. These appear as two sharp symmetric spikes in the fingerprint plots at $d_e + d_i \simeq 1.9$ and 2.4 Å in Fig. 6(*d*) and (*e*), respectively. The contribution from the other interatomic contacts summarized in Table 2 has a negligible influence on the calculated Hirshfeld surface of (I).

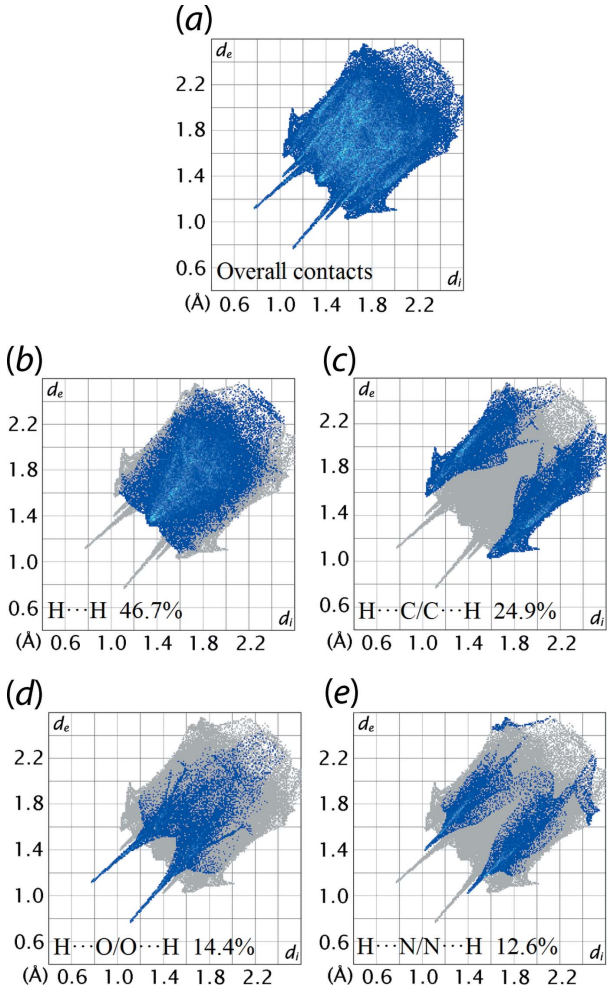

Figure 6
(*a*) The full two-dimensional fingerprint plot for (II) and (*b*)–(*e*) those delineated into H···H, H···C/C···H, H···O/O···H and H···N/N···H contacts, respectively.

Table 4
Summary of interaction energies (kJ mol^{-1}) calculated for (I).

Contact	R (Å)	E_{ele}	E_{pol}	E_{dis}	E_{rep}	E_{tot}
Intra-later						
N4—H4*N*···O2^{i}	5.21	−73.7	−14.9	−84.6	94.6	−104.2
C15—H15···O1^{iii}	5.57	−21.8	−5.7	−56.7	34.0	−55.0
C3—H3*B*···N2^{ii}	9.97	−21.4	−6.2	−20.5	25.1	−29.6
H20*B*···N3^{iv} +						
H9···O3^{v} +						
H8···H18*A*^{v}	11.43	−5.1	−1.6	−14.8	6.9	−15.2
H8···H14^{vi}	12.81	−1.4	−0.5	−9.8	2.2	−9.0
H8···H11^{vii}	9.77	−1.2	−0.4	−8.6	1.6	−8.0
H20*C*···H20*C*^{viii}	14.84	1.3	−0.2	−3.1	0.6	−1.1
Inter-layer						
H17*A*···C12^{ix}	9.37	−11.3	−3.4	−22.7	14.8	−25.1
H12···C15^{x}	10.15	−5.1	−1.2	−16.3	10.0	−14.3
H7···C5^{xi}	12.03	−3.2	−0.4	−14.0	11.5	−8.7

Notes: Symmetry operations: (i) $-x+1, -y, -z+1$; (ii) $-x+1, -y+1, -z+1$; (iii) $-x, -y+1, -z+1$; (iv) $x+1, y, z$; (v) $x-1, y, z$; (vi) $x-1, -y+\frac{1}{2}, z-\frac{1}{2}$; (vii) $-x, -y, -z+1$; (viii) $-x+2, -y, -z+1$; (ix) $x, -y+\frac{1}{2}, -z-\frac{1}{2}$; (*x*) $-x+1, y-\frac{1}{2}, -z+\frac{3}{2}$; (xi) $-x, y-\frac{1}{2}, -z+\frac{1}{2}$.

5. Energy frameworks

The pairwise interaction energies between the molecules in the crystal of (I) were calculated using the 6-31G(d,p) basis set at the B3LYP level of theory. The total energy comprises four terms, *i.e.* the electrostatic (E_{ele}), polarization (E_{pol}), dispersion (E_{dis}) and exchange-repulsion (E_{rep}) energy terms and were calculated with *Crystal Explorer 17* (Turner *et al.*, 2017). The benchmarked energies were scaled according to Mackenzie *et al.* (2017) while E_{ele}, E_{pol}, E_{dis}, and E_{rep} were scaled as 1.057, 0.740, 0.871 and 0.618, respectively (Edwards *et al.*, 2017). The energies for the identified intermolecular interactions are tabulated in Table 4. As anticipated, the greatest stabilization energy, with approximately equal contributions

from E_{ele} and E_{dis}, arises from the conventional amide-N—H4*N*···O2(carbonyl) hydrogen bond. The next most significant energies of stabilization arise from the methylene-C3—H···N2(azo) (dominated by E_{dis}) and benzene-C15—H15···O1(amide) (approximately equal contributions from E_{ele} and E_{dis}) interactions. In terms of energy, the next most significant contributions comes from an interaction in the inter-layer region, namely the H17*A*···C12 contact, Table 4. As for the other identified inter-layer contacts, E_{dis} is the dominant contributor. Views of the energy framework diagrams down *a* axis are shown in Fig. 7 and confirm the crystal to be mainly stabilized by electrostatic and dispersive forces with a clear dominance from the latter. The total E_{ele} of all pairwise interactions sum to −142.9 kJ mol^{-1}, while the total E_{dis} computes to −251.1 kJ mol^{-1}.

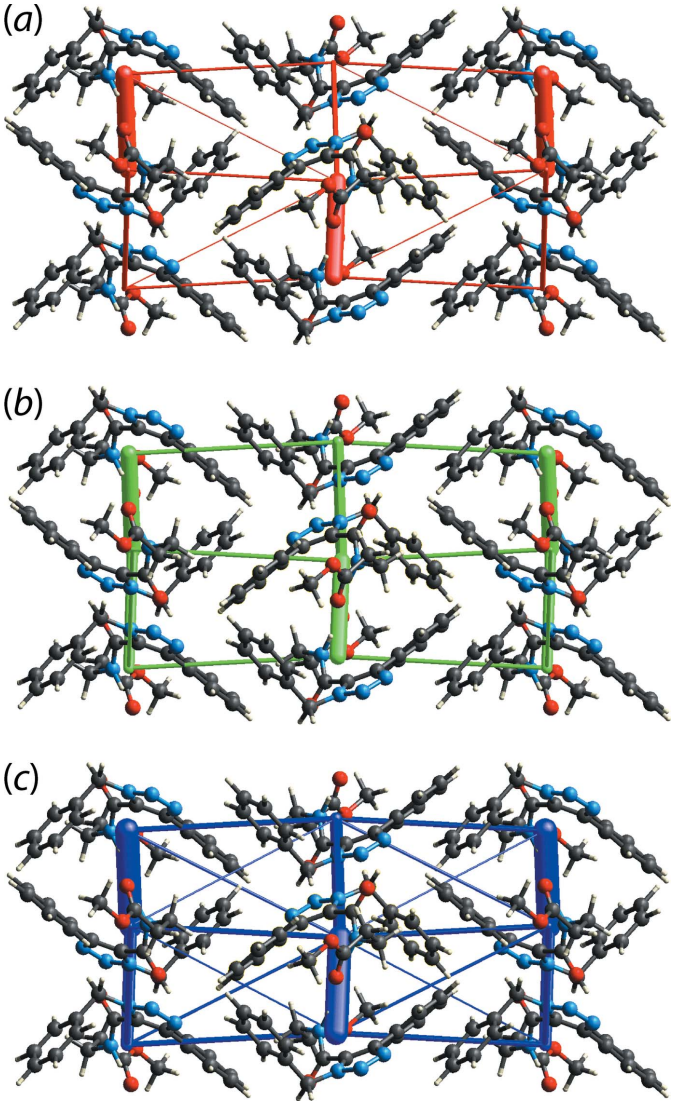

Figure 7
Perspective views of the energy frameworks calculated for (I) showing (*a*) electrostatic potential force, (*b*) dispersion force and (*c*) total energy, each plotted down the *a* axis. The radii of the cylinders are proportional to the relative magnitudes of the corresponding energies and were adjusted to the same scale factor of 50 with a cut-off value of 5 kJ mol^{-1} within 1 × 1 × 1 unit cells.

6. Database survey

There is a sole literature precedent for (I), namely the analogue with ethyl carboxylate and *N*-phenylamide substituents at the C1- and C2-atoms, respectively (WAGROM; Katritzky *et al.*, 2003), hereafter (II). An overlay diagram of (I) and (II) is given in Fig. 8. As anticipated, the five-membered rings and the α-atoms of the three substituents exhibit close concordance but, beyond this, the molecular conformations of the terminal residues differ significantly.

7. Synthesis and crystallization

Compound (I) was prepared as described in the literature (de Albuquerque *et al.*, 2019). The crystals were obtained by the slow evaporation from an ethanol solution of (I).

8. Refinement details

Crystal data, data collection and structure refinement details are summarized in Table 5. The carbon-bound H atoms were placed in calculated positions (C—H = 0.93–0.97 Å) and were included in the refinement in the riding-model approximation, with U_{iso}(H) set to 1.2–1.5U_{eq}(C). The nitrogen-bound H atom was located in a difference Fourier map and refined with N—H = 0.86±0.01 Å, and with U_{iso}(H) set to 1.2U_{eq}(N).

Acknowledgements

Regina H. A. Santos from IQSC-USP is thanked for the X-ray data collection. Ricardo S. Schwab from DQ-UFSCar is thanked for the generous gift of the sample.

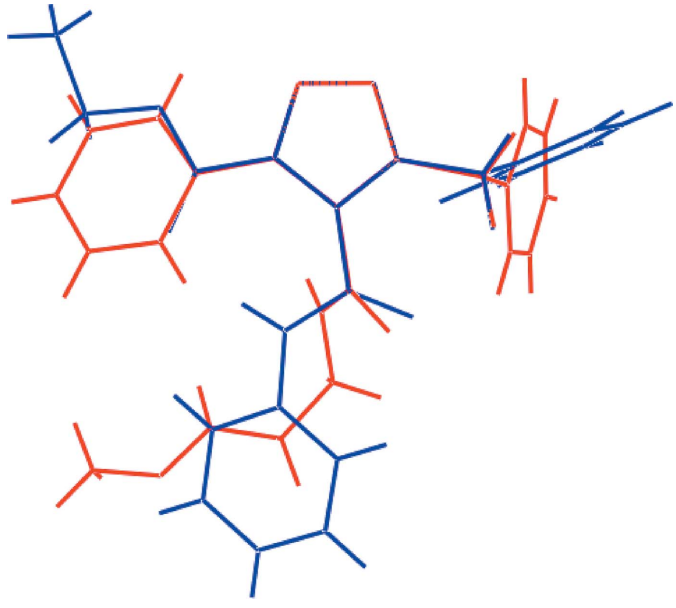

Figure 8
Overlay diagram for (I), red image, and (II), blue image. The molecules have been overlapped so the five-membered rings are superimposed.

Funding information

The Brazilian agencies Coordination for the Improvement of Higher Education Personnel, CAPES, Finance Code 001 and the National Council for Scientific and Technological Development (CNPq) are acknowledged for grants 312210/2019–1, 433957/2018–2 and 406273/2015–4 to IC, for a fellowship 303207/2017–5 to JZS. Sunway University Sdn Bhd is also thanked for funding (grant No. STR-RCTR-RCCM-001–2019).

References

Albuquerque, D. Y. de, de Moraes, J. R. & Schwab, R. S. (2019). *Eur. J. Org. Chem.* pp. 6673–6681.
Bonandi, E., Christodoulou, M. S., Fumagalli, G., Perdicchia, D., Rastelli, G. & Passarella, D. (2017). *Drug Discovery Today*, **22**, 1572–1581.
Brandenburg, K. (2006). *DIAMOND*. Crystal Impact GbR, Bonn, Germany.
Bruker (2009). *APEX2*, *SAINT* and *SADABS*. Bruker AXS Inc., Madison, Wisconsin, USA
Burla, M. C., Caliandro, R., Carrozzini, B., Cascarano, G. L., Cuocci, C., Giacovazzo, C., Mallamo, M., Mazzone, A. & Polidori, G. (2015). *J. Appl. Cryst.* **48**, 306–309.
ChemAxon (2010). *Marvinsketch.* http://www.chemaxon.com.
Edwards, A. J., Mackenzie, C. F., Spackman, P. R., Jayatilaka, D. & Spackman, M. A. (2017). *Faraday Discuss.* **203**, 93–112.
Farrugia, L. J. (2012). *J. Appl. Cryst.* **45**, 849–854.
Katritzky, A. R., Zhang, Y., Singh, S. K. & Steel, P. J. (2003). *Arkivoc*, pp. 47–64.
Mackenzie, C. F., Spackman, P. R., Jayatilaka, D. & Spackman, M. A. (2017). *IUCrJ*, **4**, 575–587.
McKinnon, J. J., Spackman, M. A. & Mitchell, A. S. (2004). *Acta Cryst.* B**60**, 627–668.
Sheldrick, G. M. (2015). *Acta Cryst.* C**71**, 3–8.
Spackman, M. A., McKinnon, J. J. & Jayatilaka, D. (2008). *CrystEngComm*, **10**, 377–388.
Tan, S. L., Jotani, M. M. & Tiekink, E. R. T. (2019). *Acta Cryst.* E**75**, 308–318.

Table 5
Experimental details.

Crystal data	
Chemical formula	$C_{20}H_{20}N_4O_3$
M_r	364.40
Crystal system, space group	Monoclinic, $P2_1/c$
Temperature (K)	293
a, b, c (Å)	11.4312 (14), 9.3013 (10), 18.737 (3)
β (°)	104.695 (4)
V (Å^3)	1927.1 (4)
Z	4
Radiation type	Mo $K\alpha$
μ (mm^{-1})	0.09
Crystal size (mm)	0.46 × 0.31 × 0.24
Data collection	
Diffractometer	Bruker APEXII CCD
Absorption correction	Multi-scan (*SADABS*; Bruker 2009)
T_{min}, T_{max}	0.544, 0.745
No. of measured, independent and observed [$I > 2\sigma(I)$] reflections	24191, 3975, 2965
R_{int}	0.066
(sin $\theta/\lambda)_{max}$ (Å^{-1})	0.628
Refinement	
$R[F^2 > 2\sigma(F^2)]$, $wR(F^2)$, S	0.077, 0.204, 1.08
No. of reflections	3975
No. of parameters	249
No. of restraints	1
H-atom treatment	H atoms treated by a mixture of independent and constrained refinement
$\Delta\rho_{max}$, $\Delta\rho_{min}$ (e Å^{-3})	0.23, −0.20

Computer programs: *APEX2* and *SAINT* (Bruker, 2009), *SIR2014* (Burla *et al.*, 2015), *SHELXL2018/3* (Sheldrick, 2015), *ORTEP-3 for Windows* (Farrugia, 2012), *DIAMOND* (Brandenburg, 2006), *MarvinSketch* (ChemAxon, 2010) and *publCIF* (Westrip, 2010).

Turner, M. J., Mckinnon, J. J., Wolff, S. K., Grimwood, D. J., Spackman, P. R., Jayatilaka, D. & Spackman, M. A. (2017). *Crystal Explorer 17*. The University of Western Australia.
Westrip, S. P. (2010). *J. Appl. Cryst.* **43**, 920–925.

supporting information

Acta Cryst. (2020). E**76**, 1051-1056 [https://doi.org/10.1107/S2056989020007380]

Methyl 3-[(1-benzyl-4-phenyl-1*H*-1,2,3-triazol-5-yl)formamido]propanoate: crystal structure, Hirshfeld surface analysis and computational chemistry

Ignez Caracelli, Julio Zukerman-Schpector, Huey Chong Kwong and Edward R. T. Tiekink

Computing details

Data collection: *APEX2* (Bruker, 2009); cell refinement: *SAINT* (Bruker, 2009); data reduction: *SAINT* (Bruker, 2009); program(s) used to solve structure: *SIR2014* (Burla *et al.*, 2015); program(s) used to refine structure: *SHELXL2018/3* (Sheldrick, 2015); molecular graphics: *ORTEP-3 for Windows* (Farrugia, 2012), *DIAMOND* (Brandenburg, 2006); software used to prepare material for publication: *MarvinSketch* (ChemAxon, 2010) and *publCIF* (Westrip, 2010).

Methyl 3-[(1-benzyl-4-phenyl-1*H*-1,2,3-triazol-5-yl)formamido]propanoate

Crystal data

$C_{20}H_{20}N_4O_3$
$M_r = 364.40$
Monoclinic, $P2_1/c$
$a = 11.4312$ (14) Å
$b = 9.3013$ (10) Å
$c = 18.737$ (3) Å
$\beta = 104.695$ (4)°
$V = 1927.1$ (4) Å^3
$Z = 4$
$F(000) = 768$
$D_x = 1.256$ Mg m^{-3}
Mo $K\alpha$ radiation, $\lambda = 0.71073$ Å
Cell parameters from 6479 reflections
$\theta = 2.5$–23.9°
$\mu = 0.09$ mm^{-1}
$T = 293$ K
Irregular, colourless
0.46 × 0.31 × 0.24 mm

Data collection

Bruker APEXII CCD diffractometer
φ and ω scans
Absorption correction: multi-scan (SADABS; Bruker 2009)
$T_{min} = 0.544$, $T_{max} = 0.745$
24191 measured reflections
3975 independent reflections
2965 reflections with $I > 2\sigma(I)$
$R_{int} = 0.066$
$\theta_{max} = 26.5°$, $\theta_{min} = 1.8°$
$h = -14\rightarrow14$
$k = -11\rightarrow11$
$l = -23\rightarrow23$

Refinement

Refinement on F^2
Least-squares matrix: full
$R[F^2 > 2\sigma(F^2)] = 0.077$
$wR(F^2) = 0.204$
$S = 1.08$
3975 reflections
249 parameters
1 restraint
Primary atom site location: structure-invariant direct methods
Secondary atom site location: difference Fourier map
Hydrogen site location: mixed
H atoms treated by a mixture of independent and constrained refinement
$w = 1/[\sigma^2(F_o^2) + (0.0396P)^2 + 3.4742P]$ where $P = (F_o^2 + 2F_c^2)/3$
$(\Delta/\sigma)_{max} < 0.001$
$\Delta\rho_{max} = 0.23$ e Å^{-3}
$\Delta\rho_{min} = -0.20$ e Å^{-3}

Extinction correction: SHELXL-2018/3 (Sheldrick 2015), $Fc^*=kFc[1+0.001xFc^2\lambda^3/\sin(2\theta)]^{-1/4}$
Extinction coefficient: 0.0267 (19)

Special details

Geometry. All esds (except the esd in the dihedral angle between two l.s. planes) are estimated using the full covariance matrix. The cell esds are taken into account individually in the estimation of esds in distances, angles and torsion angles; correlations between esds in cell parameters are only used when they are defined by crystal symmetry. An approximate (isotropic) treatment of cell esds is used for estimating esds involving l.s. planes.

Fractional atomic coordinates and isotropic or equivalent isotropic displacement parameters (Å²)

	x	*y*	*z*	U_{iso}*/U_{eq}
O1	0.3969 (2)	0.4513 (3)	0.43041 (14)	0.0558 (7)
O2	0.6787 (3)	0.0379 (3)	0.5049 (2)	0.0836 (10)
O3	0.8198 (3)	0.2035 (3)	0.5160 (2)	0.0829 (10)
N1	0.1976 (2)	0.4009 (3)	0.49963 (14)	0.0450 (7)
N2	0.1426 (3)	0.3888 (4)	0.55460 (17)	0.0635 (9)
N3	0.2173 (3)	0.3227 (4)	0.60901 (16)	0.0598 (9)
N4	0.4356 (2)	0.2164 (3)	0.45617 (14)	0.0409 (6)
H4N	0.409 (3)	0.143 (2)	0.4749 (18)	0.049*
C1	0.3218 (3)	0.2907 (3)	0.58938 (16)	0.0399 (7)
C2	0.3086 (3)	0.3412 (3)	0.51805 (16)	0.0370 (7)
C3	0.1285 (3)	0.4596 (4)	0.42786 (19)	0.0527 (9)
H3A	0.180906	0.520492	0.407502	0.063*
H3B	0.062468	0.518335	0.435328	0.063*
C4	0.0785 (3)	0.3410 (4)	0.37406 (18)	0.0482 (8)
C5	0.1396 (4)	0.2962 (5)	0.3228 (2)	0.0691 (12)
H5	0.212880	0.338684	0.321872	0.083*
C6	0.0922 (6)	0.1895 (7)	0.2736 (2)	0.0986 (19)
H6	0.133334	0.158992	0.239445	0.118*
C7	−0.0168 (7)	0.1276 (7)	0.2749 (3)	0.111 (2)
H7	−0.049067	0.054764	0.241663	0.133*
C8	−0.0772 (6)	0.1728 (6)	0.3245 (3)	0.1071 (19)
H8	−0.151197	0.131428	0.324646	0.128*
C9	−0.0299 (4)	0.2792 (5)	0.3747 (2)	0.0707 (12)
H9	−0.071464	0.308948	0.408779	0.085*
C10	0.4213 (3)	0.2167 (3)	0.64097 (16)	0.0410 (7)
C11	0.3958 (4)	0.1262 (4)	0.69416 (19)	0.0598 (10)
H11	0.316046	0.112350	0.695971	0.072*
C12	0.4876 (6)	0.0571 (5)	0.7442 (2)	0.0812 (15)
H12	0.469542	−0.003111	0.779513	0.097*
C13	0.6056 (5)	0.0765 (5)	0.7421 (2)	0.0787 (15)
H13	0.667277	0.028938	0.775749	0.094*
C14	0.6325 (4)	0.1658 (5)	0.6906 (2)	0.0679 (12)
H14	0.712690	0.179290	0.689602	0.081*
C15	0.5411 (3)	0.2367 (4)	0.63968 (18)	0.0489 (8)
H15	0.560139	0.297321	0.604805	0.059*

C16	0.3854 (3)	0.3416 (3)	0.46468 (16)	0.0357 (7)
C17	0.5073 (3)	0.1985 (4)	0.40222 (19)	0.0560 (10)
H17A	0.469697	0.251931	0.357879	0.067*
H17B	0.508059	0.097734	0.389017	0.067*
C18	0.6360 (3)	0.2500 (4)	0.4315 (2)	0.0601 (10)
H18A	0.673282	0.260002	0.390743	0.072*
H18B	0.634970	0.344092	0.453692	0.072*
C19	0.7104 (3)	0.1507 (4)	0.4873 (2)	0.0525 (9)
C20	0.9011 (5)	0.1147 (7)	0.5700 (4)	0.116 (2)
H20A	0.864583	0.092823	0.609558	0.173*
H20B	0.975609	0.165410	0.589204	0.173*
H20C	0.917047	0.027061	0.547137	0.173*

Atomic displacement parameters (Å²)

	U^{11}	U^{22}	U^{33}	U^{12}	U^{13}	U^{23}
O1	0.0565 (15)	0.0461 (14)	0.0659 (16)	−0.0003 (11)	0.0177 (12)	0.0213 (12)
O2	0.079 (2)	0.0530 (17)	0.114 (3)	−0.0147 (15)	0.0151 (18)	0.0224 (17)
O3	0.0569 (17)	0.071 (2)	0.116 (3)	−0.0102 (15)	0.0128 (17)	0.0251 (18)
N1	0.0430 (15)	0.0491 (16)	0.0420 (14)	0.0096 (13)	0.0092 (12)	−0.0051 (12)
N2	0.0502 (18)	0.092 (3)	0.0525 (18)	0.0146 (18)	0.0204 (15)	−0.0114 (18)
N3	0.0558 (18)	0.082 (2)	0.0465 (17)	0.0083 (17)	0.0218 (14)	−0.0051 (16)
N4	0.0478 (15)	0.0374 (14)	0.0422 (14)	−0.0016 (12)	0.0203 (12)	0.0002 (12)
C1	0.0442 (17)	0.0411 (17)	0.0365 (15)	0.0006 (14)	0.0140 (13)	−0.0057 (13)
C2	0.0396 (16)	0.0311 (15)	0.0399 (16)	0.0042 (13)	0.0094 (12)	−0.0019 (13)
C3	0.050 (2)	0.048 (2)	0.055 (2)	0.0155 (16)	0.0042 (16)	0.0014 (16)
C4	0.0507 (19)	0.0495 (19)	0.0407 (17)	0.0144 (16)	0.0048 (14)	0.0016 (15)
C5	0.076 (3)	0.084 (3)	0.049 (2)	0.021 (2)	0.018 (2)	0.001 (2)
C6	0.128 (5)	0.113 (5)	0.048 (2)	0.037 (4)	0.009 (3)	−0.024 (3)
C7	0.133 (5)	0.096 (4)	0.079 (4)	0.006 (4)	−0.019 (4)	−0.041 (3)
C8	0.108 (4)	0.094 (4)	0.104 (4)	−0.032 (3)	−0.001 (4)	−0.024 (4)
C9	0.062 (3)	0.082 (3)	0.064 (2)	−0.007 (2)	0.009 (2)	−0.014 (2)
C10	0.059 (2)	0.0350 (16)	0.0297 (14)	0.0017 (14)	0.0129 (13)	−0.0044 (12)
C11	0.093 (3)	0.052 (2)	0.0417 (19)	0.000 (2)	0.0307 (19)	0.0006 (16)
C12	0.148 (5)	0.060 (3)	0.042 (2)	0.021 (3)	0.035 (3)	0.0155 (19)
C13	0.119 (4)	0.070 (3)	0.038 (2)	0.037 (3)	0.002 (2)	0.0025 (19)
C14	0.064 (2)	0.078 (3)	0.052 (2)	0.019 (2)	−0.0025 (18)	−0.005 (2)
C15	0.057 (2)	0.048 (2)	0.0388 (17)	0.0015 (16)	0.0058 (15)	0.0003 (15)
C16	0.0341 (15)	0.0349 (16)	0.0360 (15)	−0.0021 (13)	0.0053 (12)	0.0029 (13)
C17	0.059 (2)	0.069 (2)	0.0475 (19)	0.0052 (19)	0.0267 (17)	−0.0019 (17)
C18	0.058 (2)	0.059 (2)	0.072 (2)	0.0023 (19)	0.034 (2)	0.015 (2)
C19	0.055 (2)	0.044 (2)	0.066 (2)	−0.0056 (17)	0.0293 (18)	0.0014 (17)
C20	0.068 (3)	0.119 (5)	0.145 (5)	0.011 (3)	0.000 (3)	0.036 (4)

Geometric parameters (Å, º)

O1—C16	1.231 (4)	C7—H7	0.9300
O2—C19	1.184 (4)	C8—C9	1.378 (7)

O3—C19	1.324 (5)	C8—H8	0.9300
O3—C20	1.446 (6)	C9—H9	0.9300
N1—N2	1.341 (4)	C10—C15	1.388 (5)
N1—C2	1.347 (4)	C10—C11	1.391 (5)
N1—C3	1.480 (4)	C11—C12	1.376 (6)
N2—N3	1.306 (4)	C11—H11	0.9300
N3—C1	1.368 (4)	C12—C13	1.371 (7)
N4—C16	1.326 (4)	C12—H12	0.9300
N4—C17	1.464 (4)	C13—C14	1.366 (6)
N4—H4N	0.860 (10)	C13—H13	0.9300
C1—C2	1.388 (4)	C14—C15	1.389 (5)
C1—C10	1.464 (4)	C14—H14	0.9300
C2—C16	1.489 (4)	C15—H15	0.9300
C3—C4	1.506 (5)	C17—C18	1.511 (5)
C3—H3A	0.9700	C17—H17A	0.9700
C3—H3B	0.9700	C17—H17B	0.9700
C4—C9	1.368 (5)	C18—C19	1.489 (5)
C4—C5	1.387 (5)	C18—H18A	0.9700
C5—C6	1.370 (7)	C18—H18B	0.9700
C5—H5	0.9300	C20—H20A	0.9600
C6—C7	1.378 (8)	C20—H20B	0.9600
C6—H6	0.9300	C20—H20C	0.9600
C7—C8	1.358 (8)		

C19—O3—C20	116.5 (4)	C11—C10—C1	119.2 (3)
N2—N1—C2	111.3 (3)	C12—C11—C10	120.5 (4)
N2—N1—C3	118.9 (3)	C12—C11—H11	119.7
C2—N1—C3	129.5 (3)	C10—C11—H11	119.7
N3—N2—N1	107.3 (3)	C13—C12—C11	120.3 (4)
N2—N3—C1	109.6 (3)	C13—C12—H12	119.8
C16—N4—C17	121.3 (3)	C11—C12—H12	119.8
C16—N4—H4N	116 (2)	C14—C13—C12	120.0 (4)
C17—N4—H4N	121 (2)	C14—C13—H13	120.0
N3—C1—C2	107.2 (3)	C12—C13—H13	120.0
N3—C1—C10	120.6 (3)	C13—C14—C15	120.6 (4)
C2—C1—C10	132.1 (3)	C13—C14—H14	119.7
N1—C2—C1	104.6 (3)	C15—C14—H14	119.7
N1—C2—C16	120.3 (3)	C10—C15—C14	119.9 (4)
C1—C2—C16	135.2 (3)	C10—C15—H15	120.1
N1—C3—C4	111.3 (3)	C14—C15—H15	120.1
N1—C3—H3A	109.4	O1—C16—N4	123.9 (3)
C4—C3—H3A	109.4	O1—C16—C2	120.8 (3)
N1—C3—H3B	109.4	N4—C16—C2	115.2 (3)
C4—C3—H3B	109.4	N4—C17—C18	112.1 (3)
H3A—C3—H3B	108.0	N4—C17—H17A	109.2
C9—C4—C5	119.7 (4)	C18—C17—H17A	109.2
C9—C4—C3	119.5 (3)	N4—C17—H17B	109.2
C5—C4—C3	120.7 (4)	C18—C17—H17B	109.2

C6—C5—C4	120.0 (5)	H17A—C17—H17B	107.9
C6—C5—H5	120.0	C19—C18—C17	112.9 (3)
C4—C5—H5	120.0	C19—C18—H18A	109.0
C5—C6—C7	119.8 (5)	C17—C18—H18A	109.0
C5—C6—H6	120.1	C19—C18—H18B	109.0
C7—C6—H6	120.1	C17—C18—H18B	109.0
C8—C7—C6	120.0 (5)	H18A—C18—H18B	107.8
C8—C7—H7	120.0	O2—C19—O3	122.7 (4)
C6—C7—H7	120.0	O2—C19—C18	125.7 (4)
C7—C8—C9	120.7 (6)	O3—C19—C18	111.6 (3)
C7—C8—H8	119.7	O3—C20—H20A	109.5
C9—C8—H8	119.7	O3—C20—H20B	109.5
C4—C9—C8	119.7 (5)	H20A—C20—H20B	109.5
C4—C9—H9	120.1	O3—C20—H20C	109.5
C8—C9—H9	120.1	H20A—C20—H20C	109.5
C15—C10—C11	118.7 (3)	H20B—C20—H20C	109.5
C15—C10—C1	122.0 (3)		

C2—N1—N2—N3	0.5 (4)	N3—C1—C10—C15	−150.9 (3)
C3—N1—N2—N3	174.1 (3)	C2—C1—C10—C15	28.8 (5)
N1—N2—N3—C1	−0.3 (4)	N3—C1—C10—C11	27.5 (5)
N2—N3—C1—C2	−0.1 (4)	C2—C1—C10—C11	−152.8 (4)
N2—N3—C1—C10	179.6 (3)	C15—C10—C11—C12	−0.5 (5)
N2—N1—C2—C1	−0.6 (4)	C1—C10—C11—C12	−178.9 (3)
C3—N1—C2—C1	−173.3 (3)	C10—C11—C12—C13	0.0 (6)
N2—N1—C2—C16	179.6 (3)	C11—C12—C13—C14	0.5 (7)
C3—N1—C2—C16	6.8 (5)	C12—C13—C14—C15	−0.5 (6)
N3—C1—C2—N1	0.4 (4)	C11—C10—C15—C14	0.5 (5)
C10—C1—C2—N1	−179.3 (3)	C1—C10—C15—C14	178.9 (3)
N3—C1—C2—C16	−179.8 (3)	C13—C14—C15—C10	0.0 (6)
C10—C1—C2—C16	0.6 (6)	C17—N4—C16—O1	−2.0 (5)
N2—N1—C3—C4	−97.4 (4)	C17—N4—C16—C2	176.2 (3)
C2—N1—C3—C4	74.8 (5)	N1—C2—C16—O1	46.0 (4)
N1—C3—C4—C9	85.4 (4)	C1—C2—C16—O1	−133.9 (4)
N1—C3—C4—C5	−96.2 (4)	N1—C2—C16—N4	−132.3 (3)
C9—C4—C5—C6	−0.7 (6)	C1—C2—C16—N4	47.9 (5)
C3—C4—C5—C6	−179.1 (4)	C16—N4—C17—C18	82.3 (4)
C4—C5—C6—C7	0.4 (8)	N4—C17—C18—C19	73.6 (4)
C5—C6—C7—C8	0.3 (9)	C20—O3—C19—O2	0.8 (7)
C6—C7—C8—C9	−0.8 (10)	C20—O3—C19—C18	−178.9 (4)
C5—C4—C9—C8	0.2 (7)	C17—C18—C19—O2	5.0 (6)
C3—C4—C9—C8	178.6 (4)	C17—C18—C19—O3	−175.4 (3)
C7—C8—C9—C4	0.6 (9)		

Hydrogen-bond geometry (Å, º)

*Cg*1 is the centroid of the (C10–C15) ring.

D—H···*A*	*D*—H	H···*A*	*D*···*A*	*D*—H···*A*
N4—H4*N*···O2^{i}	0.86 (3)	2.04 (3)	2.884 (4)	167 (3)
C3—H3*B*···N2^{ii}	0.97	2.55	3.495 (5)	165
C15—H15···O1^{iii}	0.93	2.51	3.335 (5)	148
C17—H17*B*···*Cg*1^{i}	0.97	2.71	3.640 (4)	161

Symmetry codes: (i) −*x*+1, −*y*, −*z*+1; (ii) −*x*, −*y*+1, −*z*+1; (iii) −*x*+1, −*y*+1, −*z*+1.